UNIVERSITY OF PLYMOUTH

PEARL

Snatch loading of a single taut moored floating wave energy converter due to focussed wave groups

Hann, Martyn; Greaves, Deborah; Raby, Alison

Published in:
Ocean Engineering

DOI:
10.1016/j.oceaneng.2014.11.011

Publication date:
2015

Document version:
Peer reviewed version

Link:
Link to publication in PEARL

Citation for published version (APA):
Hann, M., Greaves, D., & Raby, A. (2015). Snatch loading of a single taut moored floating wave energy converter due to focussed wave groups. *Ocean Engineering*, *96*(0), 258-271. https://doi.org/10.1016/j.oceaneng.2014.11.011

All content in PEARL is protected by copyright law. Author manuscripts are made available in accordance with publisher policies. Wherever possible please cite the published version using the details provided on the item record or document. In the absence of an open licence (e.g. Creative Commons), permissions for further reuse of content
should be sought from the publisher or author.

Download date: 24. Apr. 2025

Coastal defence using wave farms: The role of farm-to-coast distance

J. Abanades[1*], D. Greaves[1], G. Iglesias[1]

[1] Plymouth University, School of Marine Science and Engineering, Marine Building, Drake Circus, Plymouth PL4 8AA, UK

ABSTRACT

The location of a wave farm, and, in particular, its distance to the coast is one of the key aspects in a wave energy project. In the selection of the location a number of variables are typically taken into account, from the wave resource to the maintenance or infrastructure costs; however, the effects of the farm on the coast, which can be instrumental in mitigating storm-induced erosion and thus contribute to coastal defence, are seldom, if ever, considered. This is down partly to the inexistence of an *ad hoc* methodology. In this context, the objective of this work is to examine the influence of the farm-to-coast distance through a sensitivity analysis focused on Perranporth Beach (SW England). The impacts on the wave conditions and the beach morphology of a wave farm are examined in four scenarios, corresponding to three different distances from the coastline plus the baseline. A high-resolution suite of numerical models is used to study the response of the beach under different storm conditions. The results show that a wave farm closest to the beach would offer a higher degree of coastal protection than the other two scenarios, with a reduction of up to 20% in the beach erosion. The downside of this enhanced coastal protection is that the overall wave resource available at this location would be slightly smaller (approx. 10 %) than in the case of the wave farm furthest from the coast. Beyond the detailed quantitative results, the general conclusion that can be drawn is that the farm-to-coast distance is a critical variable in

*Corresponding author; e-mail: javier.abanadestercero@plymouth.ac.uk; tel.: +44.(0)7583 544041.

determining the response of a sandy beach in the lee of the farm, and should be accordingly heeded in applying a wave farm for coastal defence.

Keywords: Wave energy; Wave farm; Nearshore impact; Beach morphology; Erosion; Sediment transport

1. INTRODUCTION

The importance of wave energy is reflected in the number of very active research lines: the resource characterisation (Bernhoff et al., 2006; Carballo et al., 2014; Defne et al., 2009; Folley and Whittaker, 2009; Gonçalves et al., 2014a; Gonçalves et al., 2014b; Guedes Soares et al., 2014; Iglesias and Carballo, 2009; Iglesias and Carballo, 2010a; Iglesias et al., 2009; Liberti et al., 2013; Pontes et al., 1998; Pontes et al., 1996; Rusu and Guedes Soares, 2012; Stopa et al., 2011; Stoutenburg et al., 2010; Veigas et al.; Vicinanza et al., 2013), the technology development (Drew et al., 2009; El Marjani et al., 2008; Falcão, 2002; Falcão and Justino, 1999; Fernandez et al., 2012; Kofoed et al., 2006; López and Iglesias, 2014; López et al., 2014; Pelc and Fujita, 2002; Sahinkaya et al., 2009; Tedd and Kofoed, 2009; Thorpe, 1999; Wolgamot et al., 2012) or the environmental impacts (Babarit, 2010; Babarit, 2013; Beels et al., 2010; Bento et al., 2014; Boehlert and Gill, 2010; Mendoza et al., 2014; Millar et al., 2007; Monk et al., 2013; Palha et al., 2010; Reeve et al., 2011; Rusu and Guedes Soares, 2013; Smith et al., 2012; Veigas et al.; Veigas and Iglesias, 2013; Vidal et al., 2007; Zanuttigh and Angelelli, 2013). Conventionally, the main criterion to establish the optimum location for wave farms was the maximisation of wave power (Iglesias and Carballo, 2010b; Iglesias and Carballo, 2011), and other important aspects were often disregarded, such as the effects on the nearshore wave conditions (Carballo and Iglesias, 2013; Iglesias and Carballo, 2014) and, in particular, the eventual contribution to coastal protection provided by a wave farm. Abanades et al. (2014) proved that a nearshore wave farm reduced the erosion at the beach face by as much as 35% after storm events due to the extraction of wave energy by Wave Energy Converters (WECs). On this basis, the objective of this work is to establish the dependence of the degree of coastal protection offered by the farm on its distance from the coastline by means of a sensitivity analysis.

To accomplish this objective, four scenarios are compared, corresponding to three locations of the wave farm at different distances from the coast, plus the baseline (no farm) scenario, under different wave conditions. First, the impacts of the wave farm on the wave conditions are examined using a nearshore wave propagation model, SWAN (Booij et al., 1996). This is a phase-averaged spectral model that computes the effects of the wave farm using an energy transmission coefficient, whose values are obtained from the laboratory tests carried out by Fernandez et al. (2012). The wave farm is implemented on a high-resolution grid at different distances from a reference (10 m water depth) contour: (i) 2 km, (ii) 4 km; and (iii) 6 km. Second, based on the results of the aforementioned scenarios a coastal processes model, XBeach (Roelvink et al., 2006), is used to compare the effects of the wave farm at the different locations with the baseline scenario. A set of impact indicators is developed, specifically, to quantify these effects and establish the role played by the farm-to-coast distance.

This methodology is applied to a case study at Perranporth Beach, Cornwall (UK). A 3.5 km long sandy beach facing directly toward the North Atlantic Ocean, Perranporth is in an area with a great potential for marine renewable energy (Thorpe, 2001) – as corroborated by the Wave Hub pilot test site. The extremely energetic storms of February 2014 proved that Perranporth is subject to increased erosion risks from rising sea level and storminess (CISCAG, 2011). In view of these risks, and given that a wave farm consisting of floating WECs adapts naturally to any sea level changes (Martinelli et al., 2008), Perranporth constitutes a prime area for using such wave farms for coastal protection.

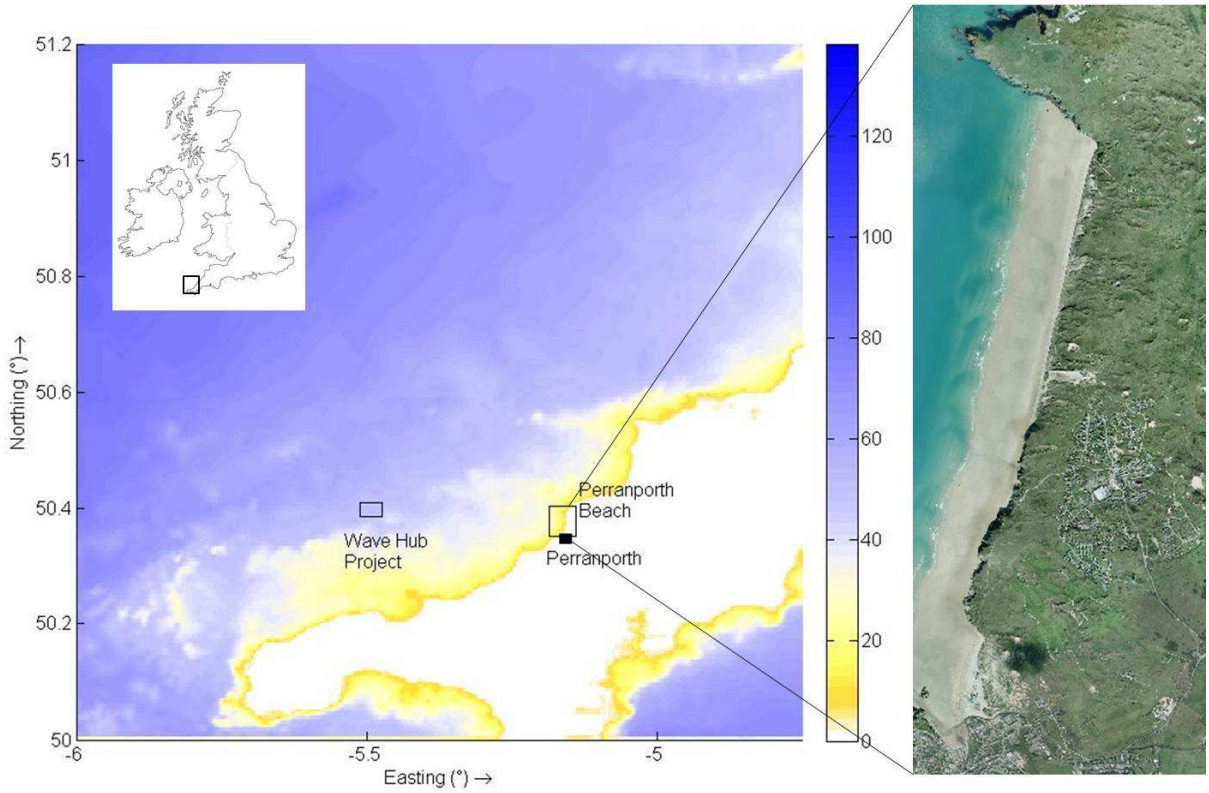

Figure 1: Bathymetry of SW England [water depths in m] including the location of Perranporth Beach, Wave Hub Project and an aerial photo of Perranporth Beach [source: Coastal Channel Observatory].

2. MATERIALS AND METHODS

2.1 WAVE PROPAGATION MODEL

The wave propagation was computed using SWAN (Simulating WAves Nearshore), a third-generation spectral wave model based on the action balance equation (Holthuijsen, 2007):

$$\frac{\partial N}{\partial t}+\frac{\partial\left(c_x N\right)}{\partial x}+\frac{\partial\left(c_y N\right)}{\partial y}+\frac{\partial\left(c_\theta N\right)}{\partial \theta}+\frac{\partial\left(c_\sigma N\right)}{\partial \sigma}=\frac{S}{\sigma} \quad (1)$$

in which the first term on the left-hand side of this equation represents the variation of wave action density (N) in time (t), the second and third term the velocity propagation in the geographical space (with c_x and c_y the propagation velocity in x- and y-space, respectively) and the fourth and fifth term the propagation velocity in the θ- and σ-space, respectively (where θ represents the direction and σ the relative frequency).

On the right-hand side of Equation (1), the source term *S* represents the effects of generation, dissipation and nonlinear wave-wave interactions.

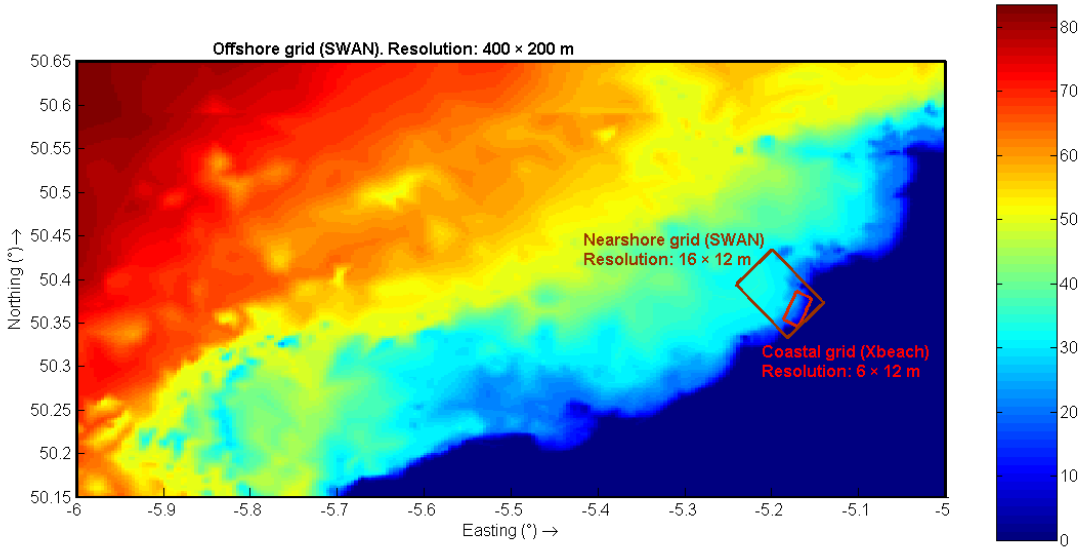

Figure 2: Computational grids of the wave propagation (SWAN) and coastal processes (XBeach) model [water depths in m]

Two computational grids with different resolutions were defined (Figure 2): (i) an offshore grid covering an area of approx. 100 km × 50 km with a grid size of 400 × 200 m, and (ii) a high-resolution nearshore (nested) grid covering the study area, with dimensions of approx. 8 km × 6 km and a grid size of 16 m × 12 m. Onto the latter grid was implemented the wave farm, which consisted of 11 WaveCat WECs (Fernandez et al., 2012; Iglesias et al., 2008) arranged in two rows, with a spacing between devices of 2.2*D*, where D = 90 m is the distance between the twin bows of a single device (Carballo and Iglesias, 2013). Two wave conditions (Table 1) were prescribed at the outer (ocean) boundary of the offshore grid based on the analysis of the offshore wave climate in the area(Kenney, 2009). Wave transmission through the wave farm was modelled following the same approach as in a previous successful application of the model (Abanades et al., 2014). For the purposes of the sensitivity analysis three locations of the wave farm were considered, at distances of 2 km, 4 km and 6 km from

the reference (10 m water depth) contour – corresponding to water depths of approx. 25 m, 30 m and 35 m, respectively (Figure 3).

Case study	H_s (m)	T_p (s)	θ (°)
CS1	3	12	315 (NW)
CS2	3.5	11	315 (NW)

Table 1: Offshore wave conditions: significant wave height (H_s), peak period (T_p) and mean direction (θ) for the different case studies.

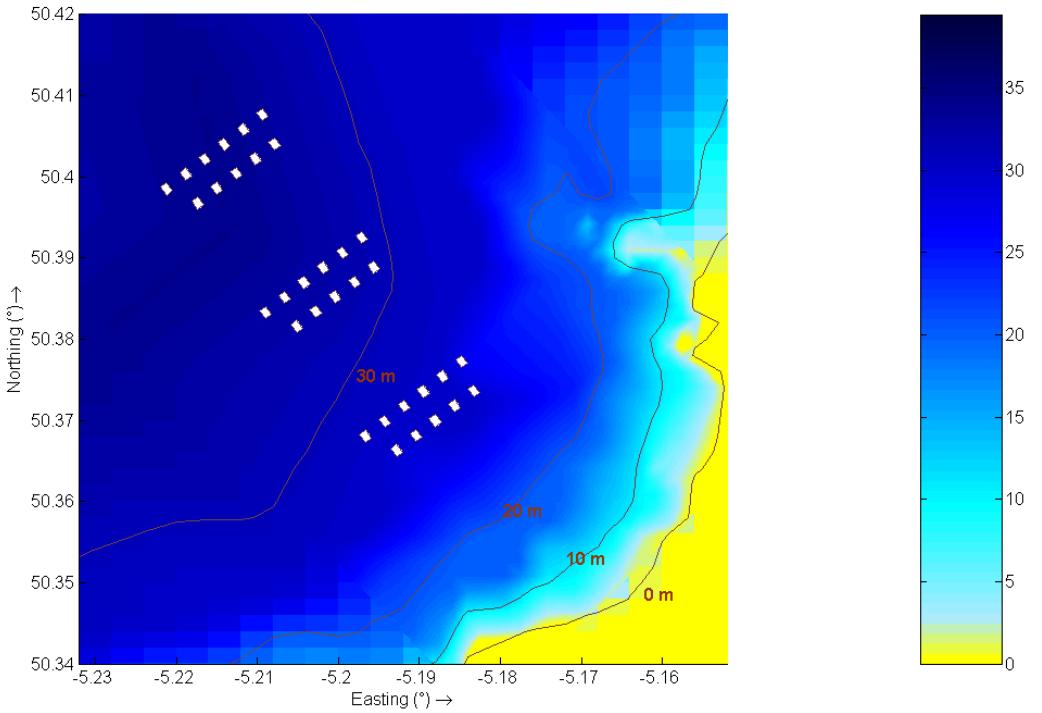

Figure 3: The three locations considered for the wave farm, at distances of 2 km, 4 km and 6 km from the reference (10 m water depth) contour [water depth in m].

To measure the impact of the wave farm on the wave conditions in its lee an impact indicator was defined: the Reduction in the Significant wave Height, RSH_i,

$$RSH_i(x,y) = H_{s,b}(x,y)^{-1}(H_{s,b}(x,y) - H_{s,f_i}(x,y)) \text{ , with } i = \text{2km, 4km or 6km,} \qquad (2)$$

where the subindex i refers to the position of the wave farm, and $H_{s,b}$ and $H_{s,fi}$ are the significant wave height in the baseline scenario and with the wave farm, respectively, at a point of the coast designated by its coordinates (x,y), with the x-

coordinate referring to the easting and the *y*-coordinate to the northing. This non-dimensional indicator quantifies the shadow caused by the wave farm in its lee.

The performance of the wave farm at the different positions was also analysed by means of the wave power (*J*, in units of Wm^{-1} in the SI), which is computed in SWAN from its x- and y-components:

$$J_x = \int_0^{2\pi} \int_0^{360} \rho g c_x E(\sigma,\theta)\, d\sigma\, d\theta \tag{3}$$

$$J_y = \int_0^{2\pi} \int_0^{360} \rho g c_y E(\sigma,\theta)\, d\sigma\, d\theta \tag{4}$$

where ρ is the water density, g is the acceleration due to gravity, and $E(\sigma,\theta)$ is the directional spectral density, which specifies how the energy is distributed over frequencies (σ) and directions (θ). The wave power magnitude is then given by

$$J = \left(J_x^2 + J_y^2\right)^{\frac{1}{2}} . \tag{5}$$

2.2 COASTAL PROCESSES MODEL

Based on the results of the wave propagation model, the coastal processes model, XBeach, was used to compute the impact of the wave farm on beach morpholology. XBeach is a 2DH (two-dimensional horizontal) time-dependent model that solves coupled cross-shore and alongshore equations for wave propagation, flow, sediment transport and bottom changes. The full description of the model can be found in Roelvink et al. (2006).

The sediment transport module solves the depth-averaged advection diffusion equation (Galappatti and Vreugdenhil, 1985) on the time scale of wave groups (Baldock et al., 2011),

$$\frac{\partial(hC)}{\partial t}+\frac{\partial(hCu^{E})}{\partial x}+\frac{\partial(hCv^{E})}{\partial y}+\frac{\partial h\left[D_{h}h\frac{\partial C}{\partial x}\right]}{\partial x}+\frac{\partial h\left[D_{h}h\frac{\partial C}{\partial y}\right]}{\partial y}=\frac{hC_{eq}-hC}{T_{S}} \quad (6)$$

where C is the wave group varying depth averaged, sediment concentration, D_h is the sediment diffusion coefficient, which is represented by an adaptation time, T_s, that is based on the local water depth, h, and sediment fall velocity. The terms u^E and v^E represents the depth-averaged velocities and C_{eq} the equilibrium concentration, representing the source term in the right hand side of the equation. The sediment transport formula defined by Van Thiel de Vries (2009) was chosen to determine the sediment equilibrium concentration.

XBeach has been widely validated to determine the impact of storms on sandy (McCall et al., 2010; Pender and Karunarathna, 2013; Roelvink et al., 2009) and gravel beaches (Jamal et al., 2014; McCall et al., 2013; McCall et al., 2012; Williams et al., 2012) at different locations. In this case, the impact of the wave farm on the beach morphology (3D) was compared to the baseline scenario at Perranporth Beach following the model set up applied by Abanades et al. (2014) at the same location to study the evolution of the beach profile (2D). The high-resolution grid implemented on XBeach covered an area of 1.4 km cross-shore and 3.0 km alongshore at Perranporth Beach with a resolution of 6 m and 12.5 m, respectively. The bathymetry data, from the Coastal Channel Observatory, were interpolated onto this grid (Figure 4), which comprised elevation values from -20 m to more than 30 m with reference to the local chart datum (LCD).

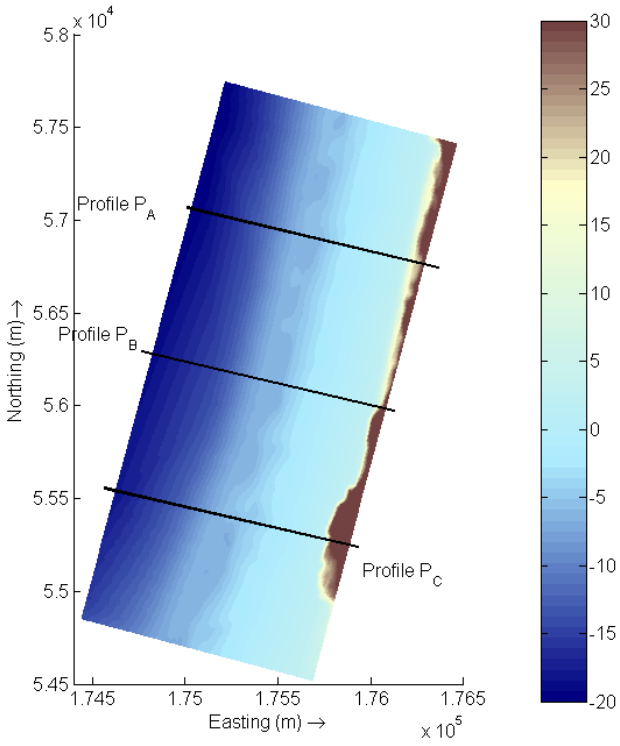

Figure 4: Bathymetry of Perranporth Beach computed in XBeach. Profiles P1, P2 and P3 included. Water depth in relation to local chart datum [in m].

The following parameters obtained from the wave propagation model along the line A-A' (Figure 5) were the input of XBeach for the analysis of the beach response under the storm events: root mean square wave height (H_{rms}), mean absolute wave period (T_{m01}), mean wave direction (θ_m) and directional spreading coefficient (s). As for tidal effects, Perranporth is a macrotidal beach with a Mean Spring tidal Range, MSR, of 6.3 m (Austin et al., 2010), and consequently their influence on the response of the beach ought to be considered (Masselink and Short, 1993). The MSR was included in the model with a semi-diurnal tidal regime (two low and two high tides each day).

The effects of the wave farm on the beach morphology were determined based on a comparison of the different wave farm scenarios with the baseline (no farm) case. The following impact indicators were defined: (i) bed level impact (BLI_i), (ii) beach face eroded area (FEA_b or FEA_i), (iii) non-dimensional erosion reduction (NER_i), and (iv) mean cumulative eroded area (CEA_b or CEA_i). The indicators corresponding to the

baseline and wave farm scenarios were denoted with the subscripts *b* or *i*, respectively, with *i* indicating the farm-to-coast distance (*i* = 2km, 4km or 6km).

The bed level impact *(BLI_i),* with units of m in the S.I., was defined as

$$BLI_i(x,y) = \zeta_{f,i}(x,y) - \zeta_b(x,y), \text{ with } i = 2\text{km, 4km or 6km,} \tag{7}$$

where $\zeta_{f,i}(x,y)$ and $\zeta_b(x,y)$ are the seabed level in the wave farm and baseline scenarios, respectively, at a generic point of the beach designated by its coordinates (*x*,*y*) in the horizontal reference plane. The *y*-coordinate axis follows the general orientation of the beach, with values increasing towards the northern end of the beach, and the *x*-coordinate is the horizontal coordinate along the profiles, with values increasing towards the landward end of the profile. Thus, the BLI_i indicator represents the change in bed level in the *i*-th scenario. A positive value signifies that the seabed level is higher in the presence of the wave farm.

The beach face is the area over the mean water level exposed to the action of the waves. In order to quantify the wave farm effects on this particularly relevant area of the beach, the beach face eroded area (*FEA*), with units of m^2 in the S.I., was defined in the wave farm ($FEA_{f,i}$) and baseline (FEA_b) scenarios by

$$FEA_b(y) = \int_{x_1}^{x_{\max}} [\zeta_0(x,y) - \zeta_b(x,y)]\,dx, \tag{8}$$

$$FEA_{f,i}(y) = \int_{x_1}^{x_{\max}} \left[\zeta_0(x,y) - \zeta_{f,i}(x,y)\right]dx, \text{ with } i = 2\text{km, 4km or 6km,} \tag{9}$$

where $\zeta_0(x,y)$ is the initial bed level at the point of coordinates (*x*,*y*), and x_1 and x_{max} are the values of the *x*-coordinate at the seaward end of the beach face and landward end

of the profile, respectively. These indicators are profile functions (the profile being designated by the y-coordinate) that evaluate the erosion caused by the storms at the beach face, thus enabling to compare the reduction of the erosion obtained in each of the three wave farm scenarios relative to the baseline case.

The non-dimensional erosion reduction,

$$NER_i(y) = 1 - \left(x_{\max} - x_1\right)^{-1} \int_{x_1}^{x_{\max}} \left[\zeta_0(x,y) - \zeta_{f,i}(x,y)\right]\left[\zeta_0(x,y) - \zeta_b(x,y)\right]^{-1} dx \,, \quad (10)$$

is also a profile function, in this case non-dimensional, which computes the variation in the eroded area of a generic profile (y) as a fraction of the total eroded area of the same profile brought about by the wave farm. A positive or negative value implies a reduction or increase in the eroded area, respectively, as a result of the wave farm.

Finally, the mean cumulative eroded area (CEA), with units of m^2 (or m^3 per linear metre of beach), was determined as well in the baseline scenario (CEA_b) and with the different wave farms ($CEA_{f,i}$). For its definition three reference profiles were considered: P_A, P_B and P_C (Figure 2). For each of these the beach was divided into two parts, to the north (CEA_b^N and $CEA_{f,i}^N$) and south (CEA_b^S and $CEA_{f,i}^S$) of the reference profile, and the corresponding indicators were computed from

$$CEA_b^S(x) = \left(y_P - y_0\right)^{-1} \int_{y_0}^{y_P} \int_{x_0}^{x} \left[\zeta_0(\chi,y) - \zeta_b(\chi,y)\right] d\chi\, dy \,, \quad (11)$$

$$CEA_{f,i}^S(x) = \left(y_P - y_0\right)^{-1} \int_{y_0}^{y_P} \int_{x_0}^{x} \left[\zeta_0(\chi,y) - \zeta_{f,i}(\chi,y)\right] d\chi\, dy \,, \quad (12)$$

$$CEA_b^N(x) = (y_{\max} - y_P)^{-1} \int_{y_P}^{y_{\max}} \int_{x_0}^{x} [\zeta_0(\chi, y) - \zeta_b(\chi, y)] d\chi dy \ , \quad (13)$$

$$CEA_{f,i}^N(x) = (y_{\max} - y_P)^{-1} \int_{y_P}^{y_{\max}} \int_{x_0}^{x} \left[\zeta_0(\chi, y) - \zeta_{f,i}(\chi, y)\right] d\chi dy \ , \quad (14)$$

where the integration variables χ and y correspond to integration along the profile and the beach, respectively. The integration limits along the profile are: x_0, the value of the x-coordinate corresponding to the first point of the profile (seaward end); x_{max}, the (landward) end of the profile. Along the beach, the integration limits are: y_0 and y_{max}, the values of the y-coordinate corresponding to the southernmost and northernmost points of the beach, and y_P the value corresponding to the reference profile. The *CEA* indicator represents the average cumulative eroded area of the two sections of the beach along the profile (x). A positive value signifies that the mean volume of material along the section of the beach is reduced compared with the initial situation (erosion).

3. RESULTS

First, the results obtained from the nearshore wave propagation model were analysed to study the impact of the wave farm on the wave conditions. The nearshore significant wave height (H_s) for the different scenarios (baseline and with the wave farm at distances of 2 km, 4 km and 6 km from the reference contour) is shown in Figure 5 for CS1 (Table 1). The reduction in the significant wave height in the lee of the farm caused by the energy extraction is apparent. This reduction was assessed by means of the impact indicator RSH_i (Figure 6) defined in Section 3.1. The maximum value of the indicator was achieved within the second row of WECs with values of up to 50%. At a distance of 1.5 km from the second row of devices, the reduction reached a peak of 40% due to the merging of the shadows caused by the first and the second row of devices.

However, this reduction decreased moving towards the coast due to the redistribution of the energy from the edges into the shadow caused by the wave farm. At a water depth of 10 m, the average reduction caused by the wave farm closest to the coast (2 km) was approx. 25%, whereas for the wave farm at 4 and 6 km the average reduction was approx. 15% and 9%, respectively.

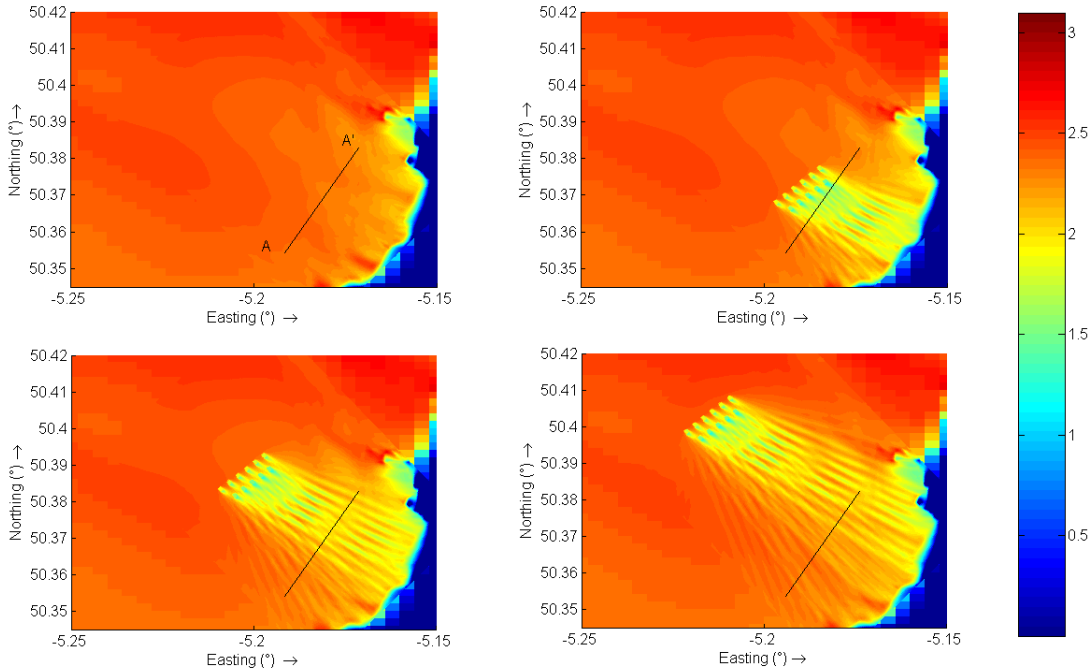

Figure 5: Significant wave height [m] in the baseline scenario and in the presence of the farm at distances of 2 km, 4 km and 6 km from the reference (10 m water depth) contour in CS1 (clockwise from above left).

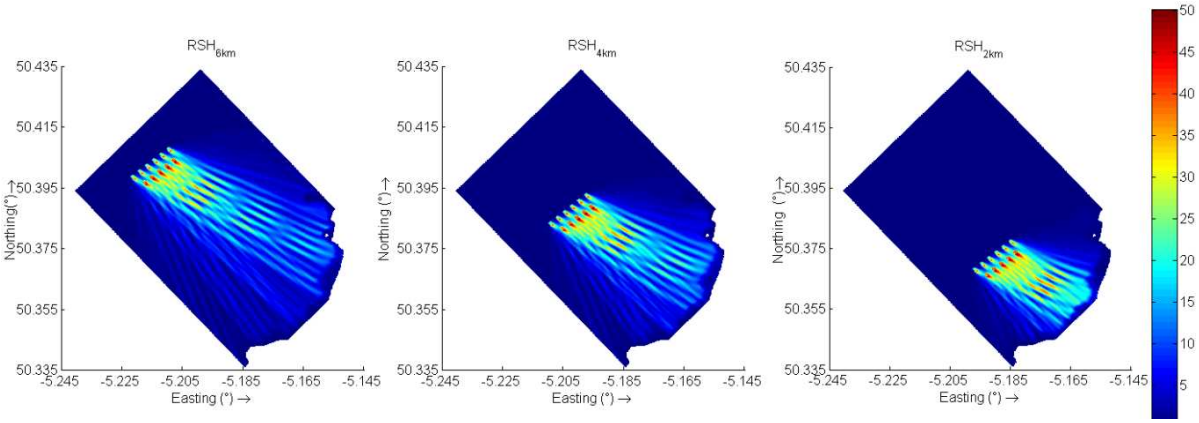

Figure 6: Reduction of the significant wave height (%) with the wave farm at a distance of: 2 km (RSH_{2km}), 4 km (RSH_{4km}) and 6 km (RSH_{6km}) from the reference (10 m water depth) contour in study CS2 [in m].

The relevance of the farm-to-coast distance may be readily observed in the shadows caused by the wave farm at different distances. The area affected at the coastline by the wave farm furthest to the coast (6 km) was greater than 7 km, however the average reduction of the significant wave height in this area was less than 5%. On the other hand, the wave farm at 2 km affected a smaller area in the coastline, around 4 km, but the reduction exceeded 10%. Figure 7 shows this reduction for CS1 (above) and CS2 (below) along the line AA´, located in Figure 5, which corresponded to the area of interest at Perranporth Beach and was used as input for the coastal processes model. This figure confirmed the different shadow pattern brought about by the wave farm at a distance of 4 and 6 km compared with the 2 km. In the latter, the reduction mainly occurred in the central section of the beach, being less significant in the northern area of the beach. However, for the other two scenarios, the reduction was found to be approx. constant along the line AA´.

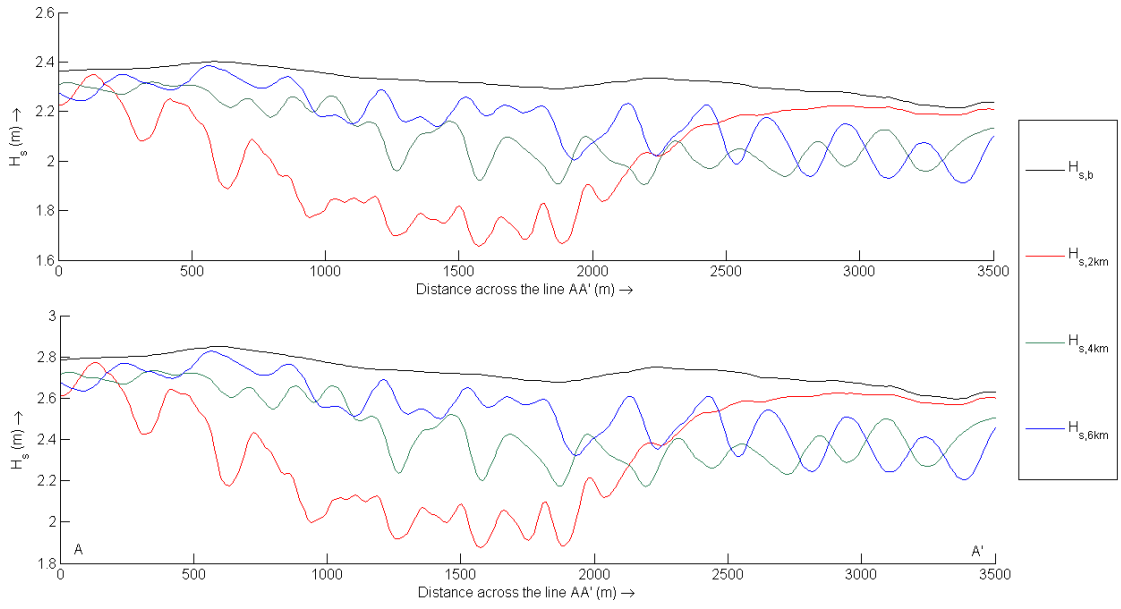

Figure 7: Significant wave height [in m] in the baseline scenario ($H_{s,b}$) and in the presence of the farm at a distance of: 2 km ($H_{s,2\,km}$), 4 km ($H_{s,4\,km}$) and 6 km ($H_{s,6\,km}$) from the reference (10 m water depth) contour across the line AA' in CS1 (above) and CS2 (below).

In terms of wave power, the resource was evaluated using equations (2), (3) and (4) at the location of each of the WECs in the wave farm. Table 2 shows the overall wave power incident on the wave farm for the different distances, it was found that the closer the wave farm to the coast, the lesser the resource, due to the dissipation caused by the different coastal processes that occur in intermediate and shallow water. For the wave farm closest to the coast the reduction of the wave power compared to the scenario with the wave farm at a distance of 6 km was 10.5% and 8.7% for CS1 and CS2, respectively. In the case of the wave farm at 4 km the reduction compared with the scenario at 6 km is 5.7% and 7.3% for CS1 and CS2, respectively. In summary, on the one hand the wave farm closest to the beach caused the greatest reduction in the significant wave height, but, on the other hand, the resource in that area is lower than in deeper areas, and, therefore, a comparative study of the response of the beach under storm conditions is necessary to determine the best location for a wave farm in terms of wave energy resource and coastal protection.

Case study (H_s)	Wave farm scenario		
	2 km	4 km	6 km
CS1: 3 m	197.52	208.02	220.75
CS2: 3.5 m	339.80	345.09	372.13

Table 2: Overall wave power incident in the wave farm [kW/m]

Second, the coastal processes model used the output of the wave propagation model to study in which manner the modification of the wave patterns affected the coastal processes and, consequently, the beach morphology. To quantify this alteration the results were analysed by means of the impact indicators defined in Section 3.2. The first indicator was the bed level difference, *BLI*, which represented the difference of the bed level between the baseline and the wave farm scenarios at a point in time. Figure 8 shows BLI values at the end of the storm for CS1 with the wave farm at a distance of 2 km (left), 4 km (middle) and 6 km (right). It was observed that the main impact caused

by the wave farm was located at the beach face, where reductions of the erosion up to 1.5 m were found.

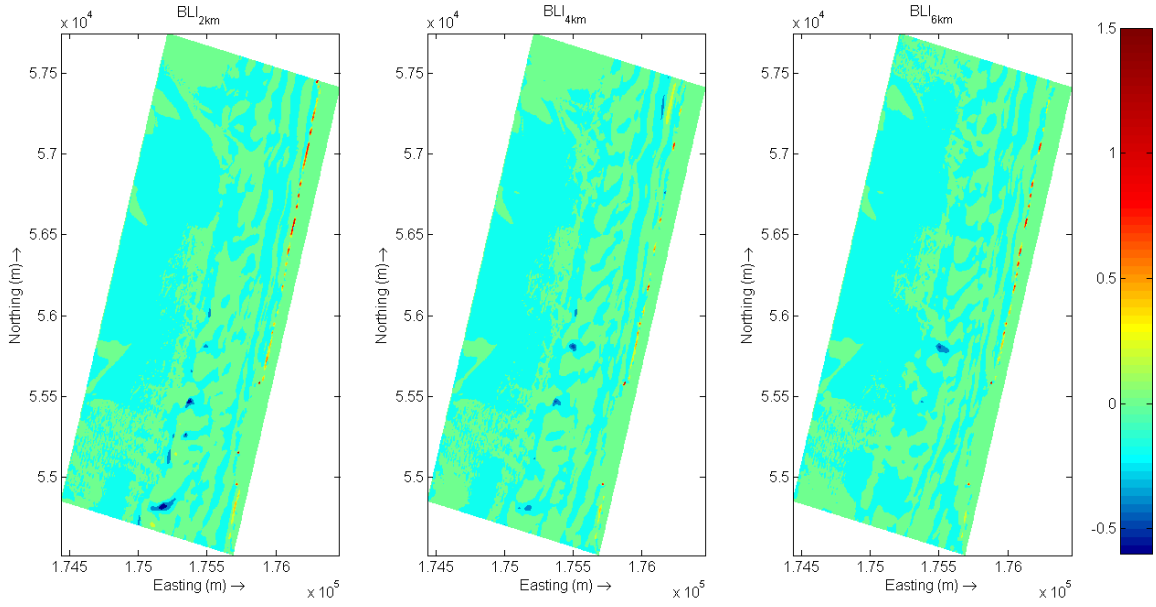

Figure 8: Bed level impact with the wave farm at a distance of 2 km (BLI_{2km}), 4 km (BLI_{4km}) and 6 km (BLI_{6km}) at the end of the storm in CS1.

Figure 9 illustrates the evolution of three profiles at the end of the storm for CS2, corresponding with three section of the beach that were identified by their different responses under the storms: (i) the southern section of the beach (P1 in Figure 9) with a smooth slope in the intertidal area; (ii) the area backed by a very steep dune (P2 in Figure 9) where the mean water level was close to the toe of the dune; and (iii) the northern section of the beach (P_3 in Figure 9) also backed by the dune, but with a greater distance from the toe of the dune to the mean water level. In the case of P_1 and P_3 the main erosion occurred on the beach face and this material was moved to lower sections of the beach, however in the case of P2 accretion was detected in the intertidal area due to the material eroded in the steep dune for the proximity of the mean water level to it.

In the area of P3 were found the greatest values of the BLI indicator, with reductions greater than 1 m, while in the section P1 the reduction took values of approx. 0.5 m.

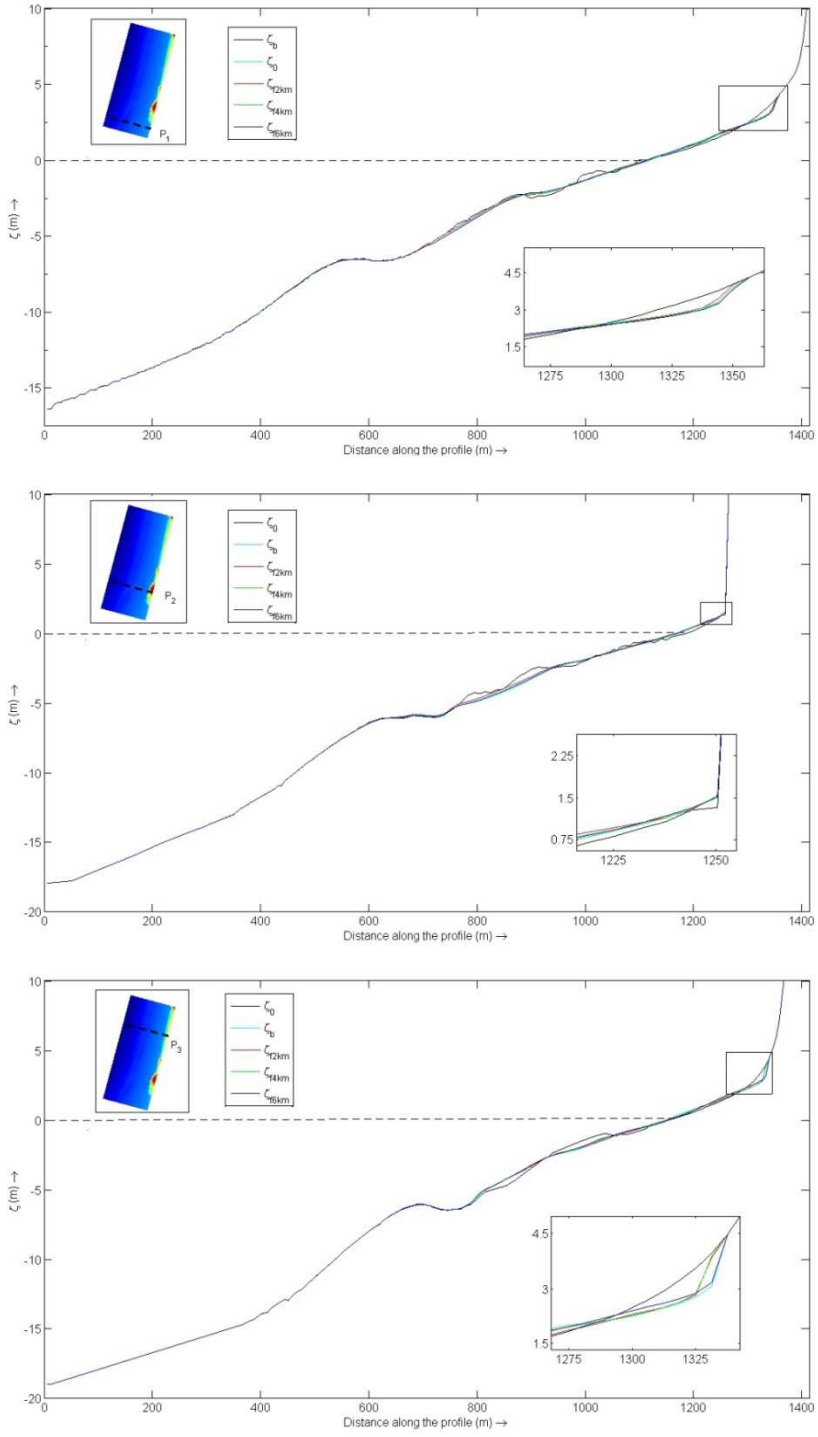

Figure 9: Bed level at Profiles P_1, P_2 and P_3: initial (ζ_0) and at the end of the storm in CS2 in the baseline scenario (ζ_b) and with the wave farm at a distance of 2 km (ζ_{f2km}), 4 km (ζ_{f4km}) and 6 km (ζ_{f6km}).

In the comparison between scenarios, the wave farm at a distance of 2 km caused greater reduction of the erosion in the beach along the beach than the other scenarios, in which areas with significant reductions of erosion were combined with negligible values or even accretion. In the lower sections of the beach, accretion occurred due to the amount of material eroded in the beach face. In the scenario with the wave farm closest to the coast the BLI took negative values of -0.5 m in the southern area of the beach, which meant that the accretion without the farm was bigger than with it, due to the greater erosion produced in the intertidal area in the baseline scenario. This reduction of the accretion with the wave farm at a distance of 4 km and 6 km took place only in a few sections of the beach with BLI values less than 0.3 m.

The impact factor FEA was defined to quantify the erosion in the beach face along the beach (Figure 10). The greatest values of this indicator along the beach were focussed in the southern area because this section was not backed by the dune. The erosion in the baseline scenario was, in general, greater than the scenarios with the wave farm, especially in the middle and northern area of the beach, *y*–coordinate (along the beach) > 1250 m. To compare the reduction between the different wave farm scenarios the indicator NER was defined, which showed the variation of the erosion in terms of the eroded area in the baseline scenario (Figure 11). The NER values fluctuated considerably along the beach, but it was observed that the reduction using a wave farm at a distance of 2 km was greater than the other two scenarios.

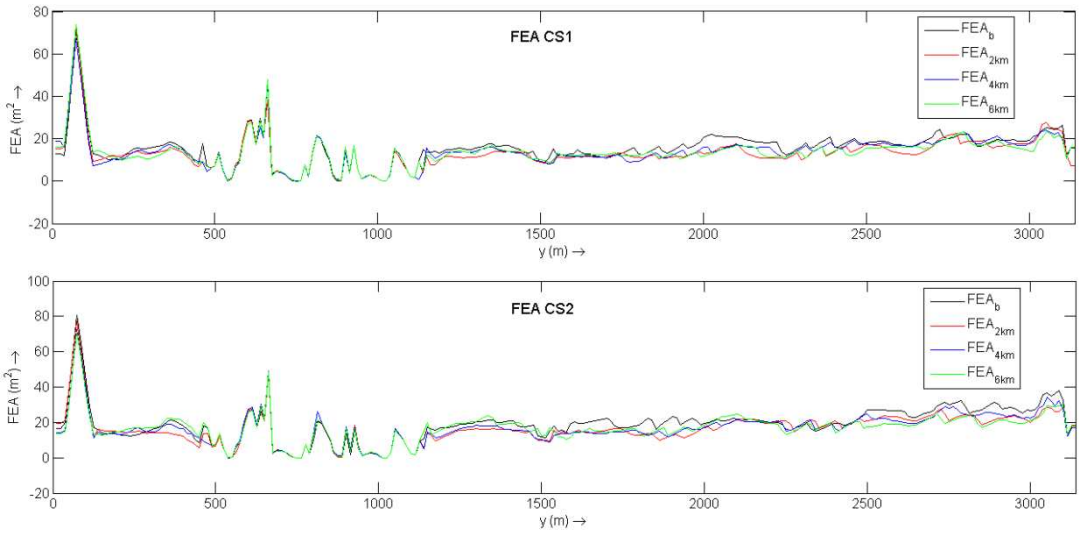

Figure 10: Beach face eroded area in the following scenarios: baseline (FEA_b) and with the wave farm at a distance of 2 km (FEA_{2km}), 4 km (FEA_{4km}) and 6 km (FEA_{6km}) along Perranporth Beach (y - coordinate, with y increasing towards the north of the beach) at the end of the storm in CS1 (above) and CS2 (below).

In the area of the steep dune (500 m < y–coordinate < 1250 m), the erosion in the beach face was very low (negligible in some sections), and very few profiles presented an isolated response taking the NER factor negative values (greater erosion with the farm than without it). However, in terms of the average reduction of the beach face erosion along the whole beach, it was confirmed that the wave farm at 2 km offered a greater degree of coastal protection, around 15% in both case studies, than the scenario with the wave farm at 4 and 6 km, which presented an approximate reduction of approx. 10%. Considering particular sections of the beach, the impact was much more significant, for instance, the reduction exceeded 20% for the wave farm at 2 km for values of the y – coordinate between 1200 and 2000 m in CS2, which was the area most affected by the reduction of the significant wave height (Figure 7). The results for the wave farm at 4 and 6 km did not present large differences in terms of the reduction of the erosion along the whole beach; however the average reduction for the farm at 4 km was slightly greater (13%) than the farm at 6 km (11%) in the area backed by the dune (y > 1250 m).

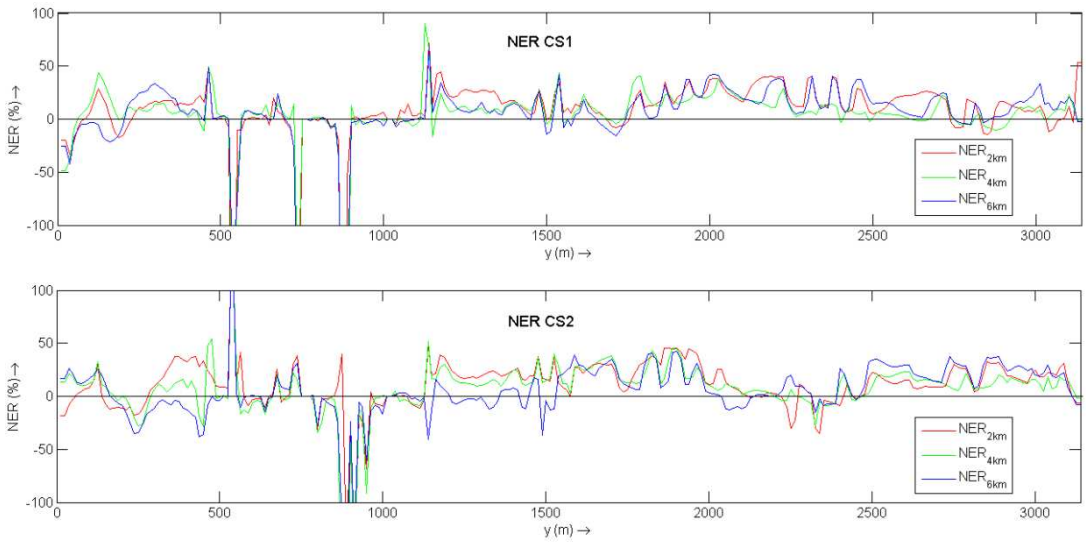

Figure 11: Non-dimensional erosion reduction (*NER*) at the beach face in the following scenarios: with the wave farm at a distance of 2 km (NER_{2km}), 4 km (NER_{4km}) and 6 km (NER_{6km}) along Perranporth Beach (*y*-coordinate, with *y* increasing towards the north of the beach) at the end of the storm in CS1 (above) and CS2 (below).

Finally, the CEA indicator computed the volume of material moved per linear metre along the beach between the initial conditions and the last point of the simulation for the different scenarios. This indicator was applied to the northern (CEA^N) and southern (CEA^S) section of the beach taking as reference for each case the following profiles (Figure 4): P_A (south), P_B (middle) and P_C (north), which allowed the variations in the longshore sediment transport to be studied. Figure 12 shows the evolution of this factor along the profile (*x*) for CS1, where the negatives values represented an increase in the volume of material with respect to the initial conditions (accretion). In the lowest section of the profile, the volume of material for the scenarios studied was larger than the initial volume due to the material eroded, mainly from the following sections along the profile: (i) the beach face (1200 m < *x*-coordinate < 1300 m) and (ii) the area that faced the storms in low tide (800 m < *x*-coordinate < 1000 m), which was more significant in the southern area of the reference profiles. The geomorphological

complexity of the southern section of the beach resulted in very different behaviour between the different scenarios.

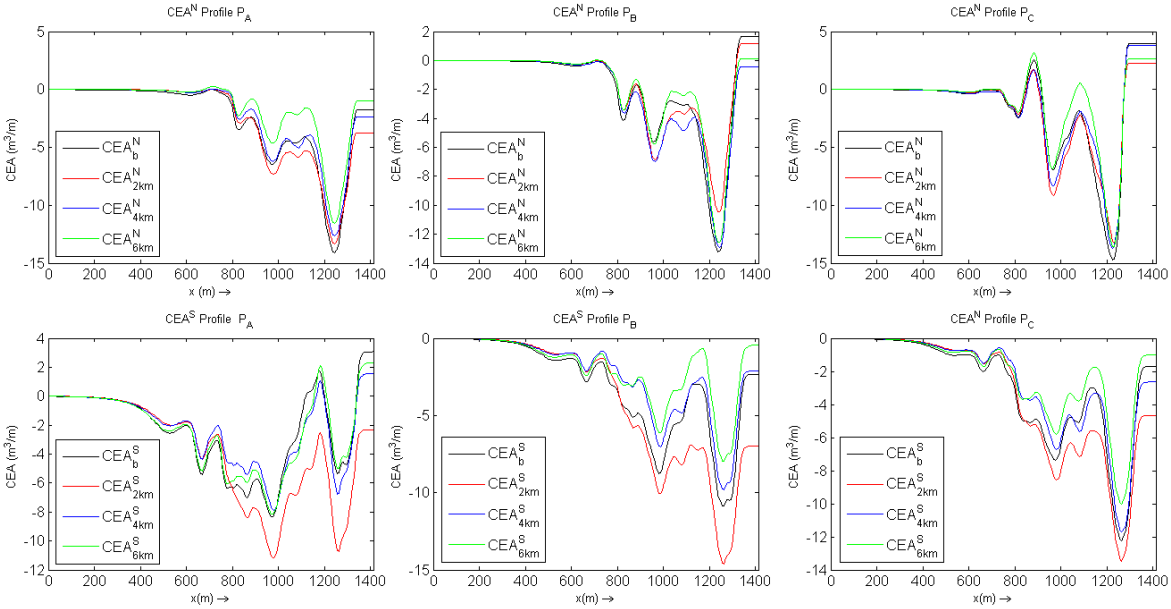

Figure 12: Mean cumulative eroded area in the baseline scenario (CEA_b) and in presence of the wave farm at a distance of 2 km (CEA_{2km}), 4 km (CEA_{4km}) and 6km (CEA_{6km}) from the reference (10 m water depth) contour in the northern area (above) and southern (below) across each of the reference profiles P_A, P_B and P_C (Figure 4) at the end of the storm in CS1. The *x*- coordinate represents the distance along the profile, with *x* = 0 the most offshore point.

The wave farm at a distance of 2 km presented a significant rise in the volume of material in the southern area of the beach, especially taking as reference the profiles P_A and P_B. This could be associated to the modification of the wave patterns brought about by the wave farm, given that the main reduction of the significant wave height occurred in the southern and middle area of the beach. Therefore, part of the material eroded in the northern section, where the reduction of the significant wave height was less, could be moved to the southern part of the beach, increasing the volume in this section. As for the wave farm at 4 and 6 km, they did not present significant differences compared with the baseline scenario, nonetheless the erosion caused in the absence of the farm was greater. For instance, in the northern area of the different profiles, it is observed that the greatest accretion at x = 1250 m occurred in the baseline scenario due to the largest

amount of material eroded at the beach face. In the case of the profile P_A, this was followed by the scenario with the wave farm at a distance of 2 km, associated with the material moved from the north of the beach, but for the profiles P_B and P_C, the greatest values of accretion, after the baseline scenario, occurred with the wave farm at 4 and 6 km given that the farm at these distances reduced the erosion less than the scenario at 2 km. To sum up, a wave farm can alter not just the wave conditions in its lee but also the morphology and the sediment transport of the beach.

4. CONCLUSIONS

The role played by the distance in the impact of a wave farm on the beach morphology was analysed in this paper. To investigate this, a wave farm formed by 11 WECs was located at different distances: 2 km, 4 km and 6 km from a reference (10 m water depth) contour in a high-resolution suite of numerical models. This suite consisted of a nearshore wave propagation model coupled to a coastal processes model, which allowed the impacts of the wave farm on wave conditions and coastal processes to be assessed.

The wave farm extracted energy from the waves, which was characterised by means of wave transmission coefficients that were obtained in laboratory tests. The comparison between the baseline and the wave farm scenarios showed the importance of the farm-to-coast distance, given that, depending on the location, the area affected by the farm and the magnitude of the wave height reduction varied considerably. In the case of the wave farm at a distance of 6 km, the impact of the farm covered an area of 7 km along the coast but the reduction of the significant wave height at a water depth of 10 m was less than 10%; nonetheless, the area affected by the wave farm closest to the

farm was 4 km and the reduction approx. 25% due to less energy being diffracted into the shadow of the farm situated closer to the beach.

The impact of the wave farm on the wave conditions resulted in an alteration of the coastal processes nearshore, and therefore, of the beach morphology. To quantify this, a suite of impact indicators was developed and applied to the results of the different scenarios. The reduction of the erosion brought about by the different wave farms was mainly in two areas of the beach: (i) the area at a water depth of approx. 3 m, which faced the storms during the low tide; and (ii) the beach face of the beach. Whereas in the former, the reduction did not exceed 0.5 m, in the latter it reached 1.5 m. In the comparison between scenarios, the wave farm at 2 km offered greater reductions of the erosion than the farm at 4 and 6 km, which presented similar responses. The overall reduction of the erosion on the beach face compared to the baseline scenario was 15% for the closest wave farm and approx. 10% for the other two. These values fluctuated significantly along the beach, and in some sections, especially in the northern area of the beach, exceeded 40%.

Lastly, it was also found that the wave farm may change the distribution of sediment along the beach. The alteration of the wave conditions with the farm at 2 km modified the sediment transport patterns, increasing the volume of material moved to the southern area of the beach. This confirmed that the effects on the beach morphology of the wave farm closest to the coast were more pronounced than in the other scenarios; nevertheless, the overall wave resource in this area was 10 % less than with the case with the furthest farm (6 km) due to the attenuation of wave energy caused by the coastal processes that occur in shallow waters. When comparing the scenarios at 4 km and 6 km, the impact on the beach morphology did not present significant differences

but there were differences in the overall resource at the wave farm: 8% less at 4 km than at 6 km.

In summary, the selection of the location for a wave farm is not trivial. In this work, it has been proven that the degree of coastal protection afforded by a wave farm varies significantly as a function of its distance to the coastline. Thus, after this study, the effects of the wave farm on the coast may become one of the main considerations in this selection, not least in areas subject to erosion risks, where the wave farms can contribute considerably to coastal defence.

5. BIBLIOGRAPHY

Abanades, J., Greaves, D. and Iglesias, G., 2014. Wave farm impact on the beach profile: A case study. Coastal Engineering, 86(0): 36-44.

Austin, M. et al., 2010. Temporal observations of rip current circulation on a macro-tidal beach. Continental Shelf Research, 30(9): 1149-1165.

Babarit, A., 2010. Impact of long separating distances on the energy production of two interacting wave energy converters. Ocean Engineering, 37(8–9): 718-729.

Babarit, A., 2013. On the park effect in arrays of oscillating wave energy converters. Renewable Energy, 58(0): 68-78.

Baldock, T.E. et al., 2011. Large-scale experiments on beach profile evolution and surf and swash zone sediment transport induced by long waves, wave groups and random waves. Coastal Engineering, 58(2): 214-227.

Beels, C., Troch, P., De Backer, G., Vantorre, M. and De Rouck, J., 2010. Numerical implementation and sensitivity analysis of a wave energy converter in a time-dependent mild-slope equation model. Coastal Engineering, 57(5): 471-492.

Bento, A.R., Rusu, E., Martinho, P. and Guedes Soares, C., 2014. Assessment of the changes induced by a wave energy farm in the nearshore wave conditions. Computers & Geosciences, 71(0): 50-61.

Bernhoff, H., Sjöstedt, E. and Leijon, M., 2006. Wave energy resources in sheltered sea areas: A case study of the baltic sea. Renewable Energy, 31(13): 2164-2170.

Boehlert, G.W. and Gill, A.B., 2010. Environmental and ecological effects of ocean renewable energy development: A current synthesis.

Booij, N., Holthuijsen, L. and Ris, R., 1996. The" swan" wave model for shallow water. Coastal engineering conference, p.^pp. 668-676.

Carballo, R. and Iglesias, G., 2013. Wave farm impact based on realistic wave-wec interaction. Energy, 51: 216-229.

Carballo, R., Sánchez, M., Ramos, V., Taveira-Pinto, F. and Iglesias, G., 2014. A high resolution geospatial database for wave energy exploitation. Energy, 68(0): 572-583.

CISCAG, 2011. Shoreline management plan Cornwall and Isles of Scilly Coastal Advisory Group.

Defne, Z., Haas, K.A. and Fritz, H.M., 2009. Wave power potential along the atlantic coast of the southeastern USA. Renewable Energy, 34(10): 2197-2205.

Drew, B., Plummer, A. and Sahinkaya, M.N., 2009. A review of wave energy converter technology. Proceedings of the Institution of Mechanical Engineers, Part A: Journal of Power and Energy, 223(8): 887-902.

El Marjani, A., Castro Ruiz, F., Rodriguez, M.A. and Parra Santos, M.T., 2008. Numerical modelling in wave energy conversion systems. Energy, 33(8): 1246-1253.

Falcão, A.F.O., 2002. Wave-power absorption by a periodic linear array of oscillating water columns. Ocean Engineering, 29(10): 1163-1186.

Falcão, A.F.O. and Justino, P.A.P., 1999. Owc wave energy devices with air flow control. Ocean Engineering, 26(12): 1275-1295.

Fernandez, H. et al., 2012. The new wave energy converter wavecat: Concept and laboratory tests. Marine Structures, 29(1): 58-70.

Folley, M. and Whittaker, T., 2009. Analysis of the nearshore wave energy resource. Renewable Energy, 34(7): 1709-1715.

Galappatti, G. and Vreugdenhil, C., 1985. A depth-integrated model for suspended sediment transport. Journal of Hydraulic Research, 23(4): 359-377.

Gonçalves, M., Martinho, P. and Guedes Soares, C., 2014a. Assessment of wave energy in the canary islands. Renewable Energy, 68(0): 774-784.

Gonçalves, M., Martinho, P. and Guedes Soares, C., 2014b. Wave energy conditions in the western french coast. Renewable Energy, 62(0): 155-163.

Guedes Soares, C., Bento, A.R., Gonçalves, M., Silva, D. and Martinho, P., 2014. Numerical evaluation of the wave energy resource along the atlantic european coast. Computers & Geosciences, 71(0): 37-49.

Holthuijsen, L.H., 2007. Waves in oceanic and coastal waters. Cambridge University Press.

Iglesias, G. and Carballo, R., 2009. Wave energy potential along the death coast (spain). Energy, 34(11): 1963-1975.

Iglesias, G. and Carballo, R., 2010a. Offshore and inshore wave energy assessment: Asturias (n spain). Energy, 35(5): 1964-1972.

Iglesias, G. and Carballo, R., 2010b. Wave energy and nearshore hot spots: The case of the se bay of biscay. Renewable Energy, 35(11): 2490-2500.

Iglesias, G. and Carballo, R., 2011. Choosing the site for the first wave farm in a region: A case study in the galician southwest (spain). Energy, 36(9): 5525-5531.

Iglesias, G. and Carballo, R., 2014. Wave farm impact: The role of farm-to-coast distance. Renewable Energy, 69(0): 375-385.

Iglesias, G., Carballo, R., Castro, A. and Fraga, B., 2008. Development and design of the wavecat™ energy converter. Coastal Engineering: 3970-3982.

Iglesias, G. et al., 2009. Wave energy potential in galicia (nw spain). Renewable Energy, 34(11): 2323-2333.

Jamal, M.H., Simmonds, D.J. and Magar, V., 2014. Modelling gravel beach dynamics with xbeach. Coastal Engineering, 89(0): 20-29.

Kenney, J., 2009. Sw wave hub metocean design basis. SWRDA.[Online] Available at.

Kofoed, J.P., Frigaard, P., Friis-Madsen, E. and Sørensen, H.C., 2006. Prototype testing of the wave energy converter wave dragon. Renewable Energy, 31(2): 181-189.

Liberti, L., Carillo, A. and Sannino, G., 2013. Wave energy resource assessment in the mediterranean, the italian perspective. Renewable Energy, 50: 938-949.

López, I. and Iglesias, G., 2014. Efficiency of owc wave energy converters: A virtual laboratory. Applied Ocean Research, 44(0): 63-70.

López, I., Pereiras, B., Castro, F. and Iglesias, G., 2014. Optimisation of turbine-induced damping for an owc wave energy converter using a rans–vof numerical model. Applied Energy, 127(0): 105-114.

Martinelli, L., Ruol, P. and Zanuttigh, B., 2008. Wave basin experiments on floating breakwaters with different layouts. Applied Ocean Research, 30(3): 199-207.

Masselink, G. and Short, A.D., 1993. The effect of tide range on beach morphodynamics and morphology: A conceptual beach model. Journal of Coastal Research: 785-800.

McCall, R. et al., 2013. Predicting overwash on gravel barriers.

McCall, R.T. et al., 2012. Modelling overwash and infiltration on gravel barriers. 2012.

McCall, R.T. et al., 2010. Two-dimensional time dependent hurricane overwash and erosion modeling at santa rosa island. Coastal Engineering, 57(7): 668-683.

Mendoza, E. et al., 2014. Beach response to wave energy converter farms acting as coastal defence. Coastal Engineering, 87(0): 97-111.

Millar, D.L., Smith, H.C.M. and Reeve, D.E., 2007. Modelling analysis of the sensitivity of shoreline change to a wave farm. Ocean Engineering, 34(5-6): 884-901.

Monk, K., Zou, Q. and Conley, D., 2013. An approximate solution for the wave energy shadow in the lee of an array of overtopping type wave energy converters. Coastal Engineering, 73: 115-132.

Palha, A., Mendes, L., Fortes, C.J., Brito-Melo, A. and Sarmento, A., 2010. The impact of wave energy farms in the shoreline wave climate: Portuguese pilot zone case study using pelamis energy wave devices. Renewable Energy, 35(1): 62-77.

Pelc, R. and Fujita, R.M., 2002. Renewable energy from the ocean. Marine Policy, 26(6): 471-479.

Pender, D. and Karunarathna, H., 2013. A statistical-process based approach for modelling beach profile variability. Coastal Engineering, 81(0): 19-29.

Pontes, M. et al., 1998. The european wave energy resource. 3rd European Wave Energy Conference, Patras, Greece, p.^pp.

Pontes, M. et al., 1996. Weratlas–atlas of wave energy resource in europe. Report to the European Commission, JOULE II Programme, 96p.

Reeve, D.E. et al., 2011. An investigation of the impacts of climate change on wave energy generation: The wave hub, cornwall, uk. Renewable Energy, 36(9): 2404-2413.

Roelvink, D. et al., 2009. Modelling storm impacts on beaches, dunes and barrier islands. Coastal Engineering, 56(11–12): 1133-1152.

Roelvink, J. et al., 2006. Xbeach model description and manual. UNESCO-IHE Institute for Water Education.

Rusu, E. and Guedes Soares, C., 2013. Coastal impact induced by a pelamis wave farm operating in the portuguese nearshore. Renewable Energy, 58(0): 34-49.

Rusu, L. and Guedes Soares, C., 2012. Wave energy assessments in the azores islands. Renewable Energy, 45(0): 183-196.

Sahinkaya, M.N., Plummer, A.R. and Drew, B., 2009. A review of wave energy converter technology. Proceedings of the Institution of Mechanical Engineers, Part A: Journal of Power and Energy, 223(8): 887-902.

Smith, H.C.M., Pearce, C. and Millar, D.L., 2012. Further analysis of change in nearshore wave climate due to an offshore wave farm: An enhanced case study for the wave hub site. Renewable Energy, 40(1): 51-64.

Stopa, J.E., Cheung, K.F. and Chen, Y.-L., 2011. Assessment of wave energy resources in hawaii. Renewable Energy, 36(2): 554-567.

Stoutenburg, E.D., Jenkins, N. and Jacobson, M.Z., 2010. Power output variations of co-located offshore wind turbines and wave energy converters in california. Renewable Energy, 35(12): 2781-2791.

Tedd, J. and Kofoed, J.P., 2009. Measurements of overtopping flow time series on the wave dragon, wave energy converter. Renewable Energy, 34(3): 711-717.

Thorpe, T., 2001. The wave energy programme in the uk and the european wave energy network.

Thorpe, T.W., 1999. A brief review of wave energy. Harwell Laboratory, Energy Technology Support Unit.

Van Thiel de Vries, J., 2009. Dune erosion during storm surges. PhD Thesis Thesis, Delft University of Technology.

Veigas, M., Carballo, R. and Iglesias, G., Wave and offshore wind energy on an island. Energy for Sustainable Development(0).

Veigas, M. and Iglesias, G., 2013. Wave and offshore wind potential for the island of tenerife. Energy Conversion and Management, 76(0): 738-745.

Veigas, M., Ramos, V. and Iglesias, G., A wave farm for an island: Detailed effects on the nearshore wave climate. Energy(0).

Vicinanza, D., Contestabile, P. and Ferrante, V., 2013. Wave energy potential in the north-west of sardinia (italy). Renewable Energy, 50: 506-521.

Vidal, C., Méndez Fernando, J., Díaz, G. and Legaz, R., 2007. Impact of santoña wec installation on the littoral processes. Proceedings of the 7th European wave and tidal energy conference, Porto, Portugal.

Williams, J.J., de Alegría-Arzaburu, A.R., McCall, R.T. and Van Dongeren, A., 2012. Modelling gravel barrier profile response to combined waves and tides using xbeach: Laboratory and field results. Coastal Engineering, 63(0): 62-80.

Wolgamot, H.A., Taylor, P.H. and Eatock Taylor, R., 2012. The interaction factor and directionality in wave energy arrays. Ocean Engineering, 47(0): 65-73.

Zanuttigh, B. and Angelelli, E., 2013. Experimental investigation of floating wave energy converters for coastal protection purpose. Coastal Engineering, 80: 148-159.